Advanced microscopy techniques to assess solid-state properties of inhalation medicines

Jagdeep Shur and Robert Price*

Pharmaceutical Surface Science Research Group, Department of Pharmacy and Pharmacology, University of Bath, Bath, BA2 7AY, UK.

*Corresponding author: Robert Price

Tel: +44 (0) 1225 383644

Fax:+44 (0) 1225 386114

e-mail: r.price@bath.ac.uk.

1. Abstract

Efficient control and characterisation of the physico-chemical properties of active pharmaceutical ingredients (APIs) and excipients for orally inhaled drug products (OIDPs) are critical to successful product development. Control and reduction of risk requires the introduction of a material science based approach to product development and the use of advanced analytical tools in understanding how the solid-state properties of the input materials influence structure and product functionality. The key issues to be addressed, at a microscopic scale, are understanding how the critical quality attributes of input materials influence surface, interfacial and particulate interactions within OIDPs. This review offers an in-depth discussion on the use of advanced microscopy techniques in characterising of the solid-state properties of particulate materials for OIDPs. The review covers the fundamental principles of the techniques, instrumentation types, data interpretation and specific applications in relation to the product development of OIDPs.

Keywords: Raman chemical imaging, dry powder inhalers, metered dose inhalers, atomic force microscopy, microscopy, chemical imaging, tomography, interferometry

2. Introduction

Material scientists have an ever-increasing array of analytical tools and techniques available at their disposal to study the physical and chemical properties of active pharmaceutical ingredients (APIs) and excipients. These tools are being widely applied in the pharmaceutical industry to support product development of therapeutic medicines. Whilst the solid oral dosage tablet still forms the mainstay of drug delivery, more complex medicines, such as those based on inhalation therapies, are being developed. These complex medicines generally require the use of bespoke tools and techniques for material characterisation. This is particularly the case for particulate-based medicaments such as orally inhaled drug products (OIDPs), where an understanding of the role of the surface and interfacial properties of APIs and excipients are key to successful product development.

This understanding is critically important for the development of suspension based pressurised metered dose inhaler (MDI) and dry powder inhaler (DPI) formulations. These portable delivery systems require the manufacture of a product which are stable enough to withstand the manufacturing process and provide a long shelf life, while allowing the drug to be effectively and reproducibly dispersed for delivery to the lung. The development of formulations, which exhibit such properties, presents considerable challenges to formulators and manufacturers.

The pressurised metered dose inhaler (MDI) is the most dominant and recognised drug delivery vehicle for lung therapy [1]. This dosage form contains the active pharmaceutical ingredient (API) dissolved or suspended in the propellant or a mixture of propellants/solvents (e.g. ethanol) [2]. Owing to the low solubility of many inhaled drug substances in the propellant (HFA134a), most MDIs are formulated as suspensions. Upon actuation of the dose from a MDI, the patient must co-ordinate their breathing to transport the aerosol into the lungs [3].

In contrast, passive dry powder inhalers (DPIs) are breath-actuated devices and do not require propellants to aid the aerosolization of the APIs. Formulations for DPIs are typically prepared as homogenous adhesive interactive mixtures, comprising of micronized drug particles and a coarse excipient carrier [4]. The coarse carrier, traditionally lactose monohydrate [5], is employed within DPI formulations to improve flow properties and metering of the highly cohesive API particles [6]. The entrainment and subsequent aerosolization of the formulation is achieved using the patient's inspiratory force, which is required to elutriate the micronized API from the surface of the carrier particle for delivery to the lower airways of the respiratory tract [7]. DPI formulations are also produced as agglomerated systems consisting of pure micronised API or mixtures of API and excipients.

In suspension MDI formulations, the interfacial properties of the API particles in suspension will be dominated by the van der Waals and electrostatic double layer forces [8]. For carrier based DPI formulations, the interactive

forces between API and excipient are dominated by a composite of van der Waals, electrostatic and capillary forces [9]. The preferential surface interactions of the API particles with excipients and other components of the container closure system of these drug product adds further complexity to suspension MDI and DPI dosage forms. These surface interactions may lead to particle agglomeration, segregation or adhesion of API to the inner walls of a device, which will contribute to inconsistent drug delivery and emitted particle size distribution [10] [11] [12]. Hence, the United States Pharmacopeia (USP) requires that the particle size distribution of the fine particle mass is characterised [13]. Additionally, the guidance suggests that appropriate characterisation of the particle size distribution of the API and any excipients should be considered [14].

The use of appropriate tools for the characterisation and control of medicines and their components is a vital part of the pharmaceutical development process. Validated analytical methods are used for the formal release of excipients and medicines but additional tools may also be utilised to understand various aspects of the medicine, especially during early phase product development. This is particularly the case for analytical methods based on microscopy.

Excipients, APIs and formulated drug products are routinely evaluated by an ‘appearance’ test. Whilst this is the lowest level of scrutiny for the evaluation of a material, the test is contained in excipient and product monographs and provides useful information about a material concerning for example, colour

and particulate appearance and also in detecting any contamination. Prior to the development of particle sizing methodologies such as inertial impactors and laser light diffraction, APIs, excipients and formulations were routinely monitored using optical microscopy. Whilst this method of examination is relatively crude, subjective and does not provide relevant information regarding the aerodynamic behaviour of drug particles, current United States of America (USA) Food and Drug Administration (FDA) chemistry manufacturing, and control (CMC) guidance believe this approach should be retained for release and stability testing of OIDPs [14]. The primary reason is that visual microscopic analysis of formulations enables identification of agglomerates within the formulation, which are likely to affect formulation aerodynamic particle size and therefore therapeutic efficacy [13]. Hence, the use of basic optical microscopy is still regarded as a relevant and appropriate methodology for probing MDI and DPI formulations to maintain control of drug product performance and stability. Whilst changes in MDI and DPI aerodynamic particle size are related to the surface properties and interfacial interactions of the API and other components of the drug product [10], there remains only a limited understanding of the relationships between material properties, particle size and drug product performance. Therefore any tool, including those based on microscopy, should be utilised to investigate such relationships.

The term ‘microscopy’ was typically applied to methods that involve visualising a material not possible with the naked eye. The three key microscopy techniques widely employed in the characterisation of OIDPs are

optical microscopy, scanning electron microscopy (SEM) and scanning probe microscopy (SPM). Optical and electron microscopy techniques utilise light and electrons, respectively, to irradiate the sample of interest. In the case of optical microscopy this is achieved by wide-field irradiation of the sample of interest with light [15]. In contrast, techniques such as confocal laser scanning microscopy (CLSM) and scanning electron microscopy (SEM) utilise a fine beam of the energy source to scan over the sample [16] [17]. These techniques have enabled in-depth investigation of the surface physicochemical properties of pharmaceutical materials and dosage forms. Additionally, methods based on scanning probe microscopy (SPM), which involve the interaction of a scanning probe with the sample of interest, have enabled greater understanding of the effect of physical, chemistry and mechanical properties of surface and their role on interfacial adhesion and cohesion in metered dose inhalers (MDIs) and dry powder inhalers (DPIs) [18] [19] [20] [21] [22][23]. The utilisation of these advanced microscopy techniques in the development of OIDPs may enable the identification of critical quality attributes of raw materials, which affect the functionality of these dosage forms.

The use of advanced microscopic based techniques in studying microscopic behaviour of particles and surfaces and their influence on the macroscopic behaviour of OIDPs has been widely implemented during product development and in manufacturing. The ultimate aim in the use of these techniques is to help reduce product failures and to limit the need of conventional end-of-line testing in enabling intelligence based manufacturing.

This is critical for the development of MDIs and DPIs, where the impact of input variability must be reduced through changes to process controls. The aim of this review is to provide an overview of these advanced microscopy techniques, with a particular emphasis on their application in investigating API and excipients for the development of OIDPs.

3. Imaging Techniques in OIDP Development

The use of microscopy in the development of inhaled products is a key requirement in the USA FDA CMC guidance for the development of OIDPs [14]. The visualisation of raw materials and final formulations can be performed from the macroscale down to the nanoscale, depending on the energy source deployed. The application of microscopy to investigate surface properties of raw materials and the structure of the processed formulation has provided useful information during pharmaceutical development of inhaled products. A number of advanced techniques have also been employed. These techniques allow the analysis of individual particles and bulk particle properties. All of the techniques can be considered as destructive and range from applying stress, such as heat, vacuum etc, to the study of static individual particles. The following sections will describe some of these techniques and their application in the development of OIDPs.

3.1 Optical Microscopy

The use of traditional light microscopes requires the operator to visually discriminate between particles on the basis of their ‘appearance’ [24]. However, this approach is both operator dependent and labour intensive, and the results tend to be relatively subjective with low statistical significance, and are limited by the number of particles (sample mass) that can be evaluated

[25]. However, the use of upright and inverse microscopes with optical beam paths for incident and transmitted light, in combination with motorized sample stages and image analysis, have enabled automated investigations of large numbers of samples and large sample areas [26].

3.1.1 Bright-field and cross-polarised microscopy

Many OIDP manufacturers have adopted the use of light microscopy to characterize and control foreign particles in OIDP dosage forms. These particles are contaminants in the formulation, and manufacturers are required by USP 788 to ensure the highest levels of product purity [27]. One of the methods, described in USP 788, is microscopic particle counting by light obscuration to measure and analyse micron-range foreign particles in pharmaceutical product manufacturing. Light obscuration analysis is useful for particle counting but not for characterization. In light obscuration, a sample dose is suspended in a liquid and exposed to a laser. Particles passing through the laser will scatter or absorb the light leading to a change in voltage in the detector. The amount of voltage needed to return the detector to its original voltage increases with increasing particle size. Particles can thus be counted in specific size ranges [28]. This approach has been demonstrated by Niemann *et al*., which has shown this method meets International Pharmaceutical Aerosol Consortium on Regulation and Science (IPAC-RS) standards for the detection of foreign particles [29].

Reliable and accurate measurement of the particle shape and size of an API, excipient and final formulation is critical in the development of an OIDP. Traditionally the naked eye and simple bright-field light microscopes have been employed for the qualitative assessment of particle shape and measurement of particle size. In the development of different carrier particles of lactose for DPIs, Larhrib *et al.* measured the elongation ratio of commercial lactose and engineered crystals of lactose produced using the addition of surfactants into the crystallization medium [30]. They used an optical microscope to calculate volume weighted median diameter of the lactose crystals. In addition, the minimum Feret diameter (mF) and maximum Feret diameter (MF) were also calculated, from which the elongation ratio was measured using equation 1.

$$Elongation\ Ratio = \frac{MF}{mF} \qquad \text{(Eq. 1)}$$

These measurements were related to the flow properties, content uniformity and in vitro aerosolization performance of formulations containing lactose with different elongation ratio. It was found that increasing the elongation ratio of the carrier or drug improved the deposition profiles of salbutamol sulphate, suggesting that the more elongated particles would be more aerodynamic and favoured deep lung penetration [30].

This technique has also been utilised to characterise lactose crystals produced from different ethanol/butanol co-solvent mixtures [31]. In these investigations, a small amount of powder was dispersed on to a microscope

slide, from which the surface volume mean diameter, Feret diameters, roundness, and elongation ratios of a hundred particles were calculated using image analysis software. The elongation ratio was calculated in the same way as Lahrib *et al.* using Eq. 1, however, the roundness of the particles was calculated using equation 2:

$$Roundness = \frac{(perimeter)^2}{4\pi Area} \quad \text{(Eq. 2)}$$

Kaialy *et al*., found that the crystallised lactose particles were less elongated and more irregular in shape with rougher surfaces than commercial samples. These data where then related to the better content uniformity and aerosolization performance of formulation blends produced using crystallised lactose when compared to those produced using commercial grade lactose. A similar approach was utilised by Kaialy *et al.,* to investigate the effect of crystallising mannitol from different binary mixtures of acetone/water on the in vitro aerosolisation performance of carried based DPI formulations produced with different mannitol crystals and salbutamol sulphate. Their investigations found that the aerosolisation performance of the formulations containing the engineered mannitol had better aerosolization performance than that of the commercial mannitol formulations [32]. It was concluded that the improvement in the DPI performance could be attributed to the presence of elongated carrier particles with smooth surfaces since these are believed to have less adhesive forces between carrier and the drug resulting in easier detachment of the drug during the inhalation.

In addition to simple bright-field microscopy, the use of polarized light as an illumination technique provides valuable insight into pharmaceutical material properties [33]. Polarized light microscopy is performed using a polarizing element below the sample to produce plane polarized light and an analyser that enables total distinction of the background, which allows detection of any birefringence. Polarized light microscopy can distinguish between isotropic and anisotropic materials. Isotropic materials (e.g. gases, liquids, unstressed glasses) demonstrate the same optical properties in all directions. Anisotropic materials, in contrast, have optical properties that vary with the orientation of incident light with the crystallographic axes. They exhibit a range of refractive indices depending both on the propagation direction of light through the substance and on the vibrational plane coordinates [34]. Consequently, polarized light is very effective in investigating particle shape, particle size and in combination with image analysis the particle size distribution. Moreover, the detection of birefringence enables investigation of crystal growth and crystallinity of pharmaceutical materials [35].

Price and Young have utilised an environmentally controlled optical microscope to further explore the effects of moisture on the metastable nature of amorphous lactose [36]. They were able to observe that at 75% RH not all of the amorphous lactose particles underwent a re-crystallization event, which was suggested by a number of bulk analytical techniques such as isothermal microcalorimetery. Upon increasing the humidity to 94% RH, they were able to observe by optical microscopy that the increased partial water vapour pressure was shown to induce primary nucleation and crystal growth of these

remaining particles. They were also showed the formation of Newton ring's surrounding these crystals, which was formed by a thin film covering the crystals.

The deliquescence behaviour of spray dried unfractionated heparin (UFH) with and without leucine was also investigated using a similar environmentally controlled optical microscope [37]. In this study, optical microscopy images showed that at low humidity, spray dried UFH was agglomerated whereas co spray dried UFH with leucine appeared as a finely dispersed white powder (Fig. 1A and B). On exposure to 90 % RH, the spray-dried UFH material began to deliquesce progressively over 15 min, as shown by the growth of transparent regions (Fig. 1A'). In contrast, at the same time-point the sample of co-spray-dried UFH with leucine remained as a finely dispersed powder (Fig. 1B and B').

3.1.2 Hot-stage microscopy

In combination with a hot-stage, temperature-dependent phase transformations can be observed by optical microscopy [38]. Not only melting points but also eventual solid-state transformations can be followed. The hot stage microscope is a polarizing microscope with a compartment that is temperature controlled by a computer. A material of interest can be mounted on a microscope slide and placed into the chamber of the hot stage. By varying the temperature, the melting point of the material of interest can be determined [39].

Chan and Gonda successfully utilised hot-stage microscopy to demonstrate phase-transformation of recombinant DNase (rhDNase)-lactose co spray-dried materials [40]. They were able to show that after exposure of the material to high relative humidity the presence of birefringence in localised areas of agglomerates was observed at 161 °C, which suggested re-crystallisation of the material. This was further obviated by the disappearance of birefringence at temperatures ranging between 200 and 210 °C, which was related to the melting of the lactose component of the co spray-dried material.

In order to gain insight into the formation mechanisms of spray-dried mannitol particles, Littringer *et al*. have utilised hot stage microscopy [41]. In their investigations, they collected droplets of aqueous mannitol solutions on a glass slide which were then placed on a hot stage, preheated to 60 °C or 120 °C. They showed that the re-crystallization process began at 60 °C, at which point the material formed small acicular crystals that grew in a radial manner from several emerging nucleation centres. Droplets placed on the hot stage at 120 °C shrunk quickly due to the fast evaporation of water but most of them were observed to remain liquid and did not recrystallize, indicating that the nucleation rate is low at these conditions. They also showed that a highly supersaturated viscous solution, recrystallization occurred instantly in the presence of seed crystals or when the temperature of the hot stage was lowered by 10 °C to 20 °C. The hot stage microscopy experiments showed, that the differences in surface topography of the spray-dried particles at lab scale are based on two different crystallization processes. At low

temperatures, fine needles crystallize from the supersaturated solution resulting in smooth surfaces. In contrast, at high temperatures (around 120 °C) the mannitol solution dried quickly to a highly supersaturated, viscous liquid since the solvent evaporation rate is high and the nucleation of crystalline mannitol is limited by lack of molecular mobility. This metastable supersaturated, viscous liquid crystallizes to coarse crystals when sufficient seeds are present, resulting in particles or spheres with rough surfaces.

3.1.3 Confocal laser scanning microscopy (CLSM)

Confocal microscopy is an imaging technique employed to obtain high-resolution images and three-dimensional re-constructions. This is achieved by using a spatial pinhole to eliminate out-of-focus light in samples that are wider than the focal plane [42]. The key feature of confocal microscopy is its ability to produce high-resolution images of thick specimens at various depths. Images are taken point-by-point and reconstructed with a computer, rather than projected through an eyepiece [43].

An image is formed using CLSM when a laser beam passes a light source aperture, which is then focused by an objective lens into a small focal volume within a fluorescent specimen. A mixture of emitted fluorescent light as well as reflected laser light from the illuminated spot is then recollected by the objective lens. A beam splitter separates the light mixture by allowing only the laser light to pass through into the detection apparatus. After passing a pinhole the fluorescent light is detected by a photodiode that transforms the

light into an electrical signal that is recorded by a computer. The detector aperture obstructs the light that is not coming from the focal point, and most of the returning light is blocked by the pinhole. This results in sharper images compared to conventional fluoresence microscopy techniques and permits one to obtain images of various z axis planes (z-stacks) of the sample. As the laser scans over the plane of interest a whole image is obtained pixel by pixel and line by line. However, the brightness of a resulting image pixel corresponds to the relative intensity of detected fluorescent light. As CLSM depends on fluorescence, a sample is usually treated with fluorescent dyes to make samples visible.

The interior structure of particles of spray dried bovine serum albumin (BSA) has been previously investigated using CLSM. In this study, spray dried powders were fixed to a glass coverslip and CLSM was used to detect voids in the particle by continuous sectioning along the z-axis of the powder sample [44]. The CLSM images revealed that the spray dried samples were non-porous. In another study, Maas *et al*., successfully used CLSM to quantify the surface roughness of spray dried mannitol particles [45]. Operating a laser at 408 nm and with a lateral resolution of 120 nm, they were able to detect surface roughness down to 10 nm. The development of this approach may provide a simple quantitative technique to evaluate the surface roughness of respirable particles.

3.2 Microscopy based on the use high energy electron beams

3.2.1 Scanning electron microscopy

Scanning electron microscopy (SEM) is used to characterize particle morphology and shape. SEM achieves extremely high resolutions down to a few nanometers and has a very flexible field of view, making it a very powerful tool [46]. This form of microscopy also provides higher magnification and depth of focus compared to optical microscopy and is suitable for particles of sizes 0.1-1000 μm [47]. SEM is routinely used to investigate particle morphology and shape and structures of DPI formulations [48] [49]. Whilst these data remain largely qualitative, they do provide important information regarding the visual appearance of the dosage form that relates to product functionality.

As inhaled API particles are typically less than 5 μm, SEM has the resolution to extensively investigate the physical properties of these materials. As such, SEM has been utilised to investigate the morphology of API particles produced using different particle engineering strategies such as spray-drying [50], spray-freeze drying [51], supercritical fluid engineering [52], solution atomisation and crystallisation by sonication (SAX) [53], and controlled precipitation [54]. The morphology of API particles is known to affect the performance of OIDPs [55], and therefore, ability to investigate this property by SEM is a critical in the development of inhaled products. This is highlighted in Fig.2, which shows an array of different morphologies of budesonide particles engineering via the SAX technology.

In addition, to characterising the API particles of in DPI dosage forms, there is an increasing use of SEM to investigate lactose carrier and final formulation structure [56]. Many studies have investigated the carrier particle shape and roughness using SEM and the relationship between shape/roughness, formulation flowability and in vitro aerosolisation performance [57] [58] [59] [60] [61] [62]. Ferrari *et al* investigated the surface morphology of lactose monohydrate following modification by a wet-smoothing process [63]. Their investigations utilised SEM to measure the rugosity of the lactose by fractal descriptors. The fractal descriptor of the roughness of the lactose materials was calculated by means of gray level distribution analysis measured over the lactose particle images, which was performed with the IMAGE 1.4 program (Wayne Rasband, National Institutes of Health, Bethesda, MD) using the algorithm called the box counting method. In this process, the SEM image analysis is conducted in a fixed area selected on a flat base. By scanning on the selected area of the image, the variability of gray level as a function of the position is obtained. In this way, Ferrari *et al.* were able to demonstrate that the process of smoothing allowed the preparation of lactose particles with different degrees of surface roughness for the control of flow and packing properties and particle-particle interactions.

In addition, studies have also used SEM to investigate the role of mechanical processing on the shape and morphology of carrier lactose materials [64,65]. An example of an SEM micrograph of an adhesive DPI mixture of lactose (SV003, DMV-Fonterra, Netherlands) and budesonide is shown in Fig. 3. The

image shows the surface of the lactose, from which the surface topology of the carrier can be distinguished. Furthermore, the images shows the presence of particles of budesonide adhered to the surface of the lactose. In this way, SEM can be used to investigate the effect of mechanical processing on the size, shape and morphology of carrier particles, which may subsequently affect fine particle delivery. Similarly, the shape and morphology of different sugar carrier materials have been investigated using SEM, and has been related to powder flow properties and final drug product performance [66].

The use of as a ternary agents such as fine lactose particles in dry powder inhalers (DPI) has been widely documented, and is known to modify the performance and stability of DPI drug products [67]. SEM has been routinely utilised to investigate the affect of these ternary agents on formulation microstructure of carrier-based DPI formulations. For example, Adi *et al*., utilised SEM to investigate the effect of fine lactose particles on adhesive mixtures of lactose with salmeterol xinafoate [68]. Their examination of these mixtures by SEM demonstrated agglomeration in mixtures containing the drug and fine lactose particles. They were also able to identify by SEM that the drug adhered on the surface of the fine lactose formed agglomerates approximately 17 and 30 μm in size. Adi *et al*. also showed that carried-based formulations produced with 3.0 and 7.9 μm fine lactose particles demonstrated different packing structures, which was related to different agglomeration behaviour and accounted for the difference in dispersion behaviour.

3.2.2 Advanced scanning electron microscopy techniques

An advance on SEM technology has been the development of the environmental SEM (ESEM). The ESEM eliminates the need for many of the sample preparation treatments related to conventional SEM. In addition, samples are imaged in a partial pressure of gas, and therefore, are not directly under high vacuum [69]. High energy electron beams enter the sample and generate secondary electrons as in a SEM. Furthermore, sample do not need to be coated during ESEM investigations [70]. This has enabled the investigation of materials in their native state. Recently, Watling *et al*., have utilised ESEM to investigate the effect of different storage humidity conditions on the properties of lactose [71]. ESEM investigations were able to identify that upon storage at high humidity the particle surface became much smoother, and that the fine particle lactose may form solid bridges, which results in the coarsening of the bulk powder.

3.2.3 Focused ion beam-scanning electon microscopy (FIB-SEM)

The focused ion beam-scanning electron microscope (FIB-SEM) might be a suitable microscope to study inhaled pharmaceutical samples. This microscope has been mostly used on non-biological samples [72], although recently the FIB-SEM has also been used to study biological samples [73] [74].

The FIB-SEM combines a scanning electron microscope with a focused ion beam. At relative low magnifications the SEM mode can be used to image a large area of a sample. In addition, in scanning mode the system can navigate to zoom in and out of the areas of interest. The FIB can subsequently be used to remove small volumes of material, a process called sputtering or milling, ranging from tens of cubic nanometres up to thousands of cubic micrometres at the areas of interest. The sidewalls of the milled trenches reveal a cross-section of the sample and can be visualized in the SEM mode. This enables the elucidation of 3D information of the architecture of the sample.

Heng *et al.*, have utilised FIB-SEM to investigate the porosity of a number of spray dried powders, which consisted of bovine serum albumin (BSA), mannitol and disodium cromoglycate [75]. They conducted FIB milling of the samples using a focused ion-beam/scanning electron microscope dual beam system (Quanta 200 3D, FEI, USA). As each material had different mechanical properties the milling parameters of each material were altered using parameters such as the accelerating voltage, beam current and mill depth. Their investigations found that as the surface corrugation of spray dried BSA particles increased their porosity decreased. In addition, FIB-SEM studies suggested that spray-dried mannitol particles were porous, whereas FIB-SEM analysis of particles of spray dried disodium cromoglycate suggested the material had a porosity rate of 0 – 10 %. This study highlighted the novel used of FIB-SEM for investigating the internal structure of respirable particles, which may provide useful information regarding aerodynamic properties of particles.

3.2.4 Transmission electron microscopy

Transmission electron microscopy (TEM) is a related technology to SEM, but is rarely employed, mainly due to the demanding sample preparation and limited sample contrast. However, TEM provides the highest resolution of the electron based microscopies. Chew and Chan have demonstrated this in their investigations of spray-dried mannitol [76]. They utilized freeze-fracture to examine the interior of individual particles of spray-dried mannitol. A replica of the fracture surface was made in carbon, which was then viewed in the TEM. They were able to conclude that the spray-dried particles of mannitol were not hollow, which was contrary to the findings by the same group when they used FIB-SEM to evaluate the porosity of spray dried mannitol [75]. These findings suggest that when examining particle porosity by electron microscopy it is important to use complimentary techniques to enable through evaluation of the material of interest.

3.3 Microscopy based on the use of a scanning probe

3.3.1 Atomic Force Microscopy (AFM)

Scanning probe microscopy (SPM) is the name given to a range of techniques, which involves the formation of images and acquisition of surface properties data from a range of physical, optical and chemical interactions between a sharp proximal probe and a surface, one of which is atomic force

microscopy (AFM) [77]. In 1986, the AFM was invented by Binnig *et al.,* which allowed surfacing imaging of insulating materials at a nanoscale [78]. The AFM quickly become a routine tool for surface microscopy, offering many advantages, such as minimal sample preparation, and overcoming the need for high vacuum conditions required for high-energy electron beam microscopes [79].

In simple terms, the AFM utilises a sharp, pyramidal tip mounted on a spring-like cantilever, which is brought into close contact to the surface of interest, where the intermolecular forces acting between the tip and the surface cause the cantilever to bend [80]. Topographical images of the surface are obtained by recording the cantilever deflection, as detected by a laser beam, which is positioned at the free end of the cantilever, as the sample is rastered back and forth beneath the probe [23]. The AFM can be operated in vacuum, air or in a liquid environment.

Given the importance of interfacial forces on the blending dynamics and aerosolisation behavior of DPI formulations and suspension properties of APIs in MDIs, it is not surprising that the colloidal probe technique has been widely applied in the area of inhalation [81] [82] [83] [84] [85]. In this approach, a single micronised particle is attached to the apex of a cantilever as shown in Fig. 4. In this way, the particle is able to interact with the substrate and from which the force of adhesion maybe calculated. Force-distance curves can be generated singly, but in order to obtain a statistically relevant set of data in a single operation, force-volume mode can be employed. In this mode, the AFM

raster scans the substrate under the colloidal probe to produce a series of force-distance curves, each from a well-defined interval in the *x* and *y* direction, and a low-resolution topographical image. These data can be processed to calculate the force of adhesion from each individual force curve, which can be displayed as a force volume map, showing variation in adhesion over the surface (Fig. 5). In this way, the effect of environmental properties such as humidity on the cohesion and adhesion properties of inhaled APIs and lactose have been investigated [18] [86]. Furthermore, the adhesion of lactose fines to pharmaceutical surfaces has also been investigated to develop an understanding of the role of fine lactose on DPI formulation [87].

Investigations into the surface interfacial properties of inhaled APIs have been carried out using a wet cell AFM system, in which the medium utilised had similar properties to HFA134a, but was liquid at atmospheric pressure [88] [89-91]. In this way, the surface interfacial properties of API materials were investigated and related to their behaviour in MDI suspension systems [92].

The intrinsic roughness and irregular morphology of processed excipient and APIs in OIDP formulations, has severely limited the general use of colloid probe microscopy [93]. Most studies produced high variability in colloid probe adhesion measurements between formulation components, because it led to significant variation in the contact area between the colloidal probe and substrate, to which adhesion is directly proportional [94].

A number of experimental approaches have been developed to overcome this limitation. One such technique employs a grid of extremely sharp spikes over which the colloidal probe is scanned, resulting in reconstructed image of the interacting probe from which the morphology and the contact radius of the particle can be calculated [95]. It is then possible to normalise adhesion measurements by the radius of contact and so calculate the work of adhesion between the substrate and particle. This approach has been utilised to investigate adhesive properties of API materials processed by different technologies and to calculate the surface energy of API and excipient materials employed in MDI and DPI formulations [96] [21].

Another technique that overcomes the limitation of contact area and which has been used to explain the influence of interfacial chemistry of APIs on interfacial interactions within DPI systems is the cohesive-adhesive balance (CAB) technique [97,98]. The CAB approach employs specially grown molecularly smooth crystals as substrates to ensure that the contact area between a given colloidal probe and various substrates is uniform and constant.

A number of colloidal probes of each material under investigation are prepared and the interactive forces between each probe and a crystalline substrate of each material under investigation measured. These data are used to produce a CAB graph, by plotting the mean cohesive force for each probe (the adhesive force between a probe and a substrate of the same material) against the mean adhesive force between that probe and a

substrate of another material. When data for a number of probes of the same material interacting with the same substrate are plotted on the same axes, a straight line is formed allowing linear regression analysis of these data. Although the contact area of each probe may vary significantly, the contact area of an individual probe is the same for both the cohesive and adhesive measurements and thus the ratio between cohesion and adhesion remains consistent between different probes. This ratio (known as the CAB ratio) can be measured from the analysis of the gradient of the CAB graph.

The CAB approach to colloid probe AFM has demonstrated that the cohesion of budesonide is 1.19 times greater than its adhesion to lactose [99] [100] and the adhesion of fluticasone propionate to lactose is 4.55 times greater than the cohesion of fluticasone propionate [101]. In this way, the CAB procedure is able to produce data that are independent of the contact area between the colloidal probe and substrate and are, therefore, a quantitative analysis of the influence of interfacial chemistry on API-lactose interactions. The approach has been shown to predict the behaviour and possibly the *in vitro* performance of simple powder formulations (with and without force control agents) of binary DPI systems [102] [66] .

3.2.2 AFM Tapping-Mode® and Phase Imaging

One of the earliest AFM operating modes for imaging substrate surfaces was in the contact mode. In contact mode imaging, the tip and sample are placed in contact and the tip is rastered across the surface resulting in a

topographical image of the surface [103]. One of the key disadvantages of the contact mode is that the dragging motion of tip combined with adhesive and lateral forces, can cause substantial damage to both the tip and sample [79]. This may be problematic when imaging relatively soft pharmaceutical materials. To alleviate this problem, non-contact or intermittent modes, such as TappingMode®, have been developed. In this mode, rather than encountering repulsive forces, the cantilever is oscillated and changes in phase or amplitude are measured whilst scanning. Therefore, attractive forces between the tip and the surface are measured, which are significantly smaller than the force applied on samples in the contact mode operation [104]. This approach has enabled the measurement of surface rugosity of different APIs and excipient materials such as lactose [61], erythritol [105] and trehalose [106]. The roughness of imaged areas are quantified using the mean (*Ra*) and root mean squared roughness (*Rq*) of the variations in the height of the asperities of the imaged topographical surface, as calculated by the AFM software using equations 3 and 4.

$$R_a = \frac{1}{n_p} \sum_{i=1}^{n} |y_i| \qquad \text{(Eq. 3)}$$

$$R_q = \sqrt{\frac{1}{n_p} \sum_{i=1}^{n} y_i^2} \qquad \text{(Eq. 4)}$$

where n_p is the number of points in the image and y_i is the distance of the asperities *i* from the central line. In this way, it has been possible to calculate the roughness of lactose prepared by different surface modification processes, and the effect of materials with different roughness has been related to the performance of DPI formulations [63] [107].

The TappingMode® operation also enables the measurement of a phase signal that can give information about stiffness/elasticity, viscoelasticity and adhesion of the surface of materials. This phase signal generates a Phase image, which is acquired simultaneously as the topography image. Previous investigations of pharmaceutical systems, using phase imaging, have elucidated polymorphic variations in cimetidine crystals [108] and investigated the internal chemical structure of starch granules [109]. Phase imaging has been used to characterise the crystalline disorder (amorphous content) on the surface of micronized APIs [104]. Young and Price utilised phase imaging to investigate amorphous to crystalline transitions on the surface of lactose materials [110]. An example of AFM phase imaging is shown in Fig. 6, which shows a topographical and phase image of surface of an individual micronized particle. The image shows the presence of discrete regions, which resemble “pits/craters” over the surface. These well-defined regions produce a significant phase shift response (>100°) upon interaction with the probing tip as shown by Fig. 6, which suggests significant variation in the surface physico-mechanical properties of the material. These regions are related to regions of processed induce surface structural disorder caused by the

mechanical damage during micronization. These highly energetic sites are known to influence the surface interfacial properties of materials and their stability of the particles in suspension MDIs and DPIs.

3.2.3 White-Light Interferometry

White light interferometry has been used for many years as a reliable non-contact optical profiling system for measuring step heights and surface roughness [111]. The main disadvantage compared to AFM measurements is that the lateral resolution is limited to around 0.35μm [25]. However, white light interferometry is routinely utilised in the semiconductor industry for examining the surface roughness of semiconductor wafers [111].

The technique involves splitting an optical beam from the same source into two separate beams [25]. One of the beams is passed through, or reflected from, the object to be measured whilst the other beam (the reference) follows a known and constant optical path. A light source provides a beam, which is passed through a filter and reflected down to an objective lens. This combines the light beams reflected from the sample surface and the reference surface, which creates an interference pattern of light and dark fringes (an interferogram), which is magnified by the microscope optics and imaged by a CCD camera. As the objective lens is moved vertically between sample and beam splitter, a series of moving interference fringes which the camera will detect. The aim is to establish the point at which maximum constructive interference occurs [111]. Once this is achieved, provided the vertical

movement of the lens can be accurately tracked, it is possible to create a 3D map of the sample surface by measuring the position of the lens required to produce the brightest image at each point on the CCD array. Each pixel of the CCD array effectively acts as an individual interferometer and thus builds up a very accurate map of the surface. An example of white light interferometry for investigating the surface roughness of lactose is shown in Fig. 7. The surface roughness of ML001 (DMV-Fonterra, Netherlands) was investigated using a Veeco WYKO NT1100 (Veeco, Cambridge, UK). The surface topology of ML001 is shown in Fig. 7 and indicates that material has high surface rugosity. The Ra and Rq surface roughness measurements were 1.32 and 2.20 μm, respectively. Surfaces with such high roughness are difficult to image using AFM, and therefore, white light interferometry maybe suitable for the measurement of the surface roughness of carrier lactose.

Recently, Adi *et al*., have measured the surface roughness of the BSA and lactose particles by white-light interferometry [112]. Roughness values determined by interferometry were in good agreement with AFM-derived values. Their data suggested that the roughness of BSA particles ranged from 18 – 110 nm. In addition, the roughness of commercial lactose was determined as 300 nm, but was smaller upon decantation of the lactose. They concluded that this approach was useful for rapid evaluation of surface morphology and roughness of particles used in DPI formulations.

3.2.4 Micro-thermal analysis using scanning thermal microscopy

There has been growing interest in the physical transformation at the surfaces of pharmaceutical solids. The scanning thermal microscope (SThM) has been used to probe thermal properties of pharmaceutical materials at the sub-microscopic scale. The SThM uses nanofabricated thermal probes, with a resistive heater at the tip, to achieve unprecedented high spatial and thermal resolution and sensitivity with a unique signal detection system [113]. The SThM technique maps the thermal properties of the sample surface by holding the probe temperature constant and measuring the power required to maintain this temperature, whilst the probe or sample is being rastered. As the probe encounters an area of the sample with high thermal conductivity more heat is lost from the tip of the probe to the sample and thus more power is required to maintain a constant temperature. In this way, the thermal conductivity of a sample surface can be mapped.

Harding *et al*., have utilised SThM to discriminate between amorphous and crystalline indomethacin material on a sub-micron scale [114]. They were able to achieve submicron lateral spatial resolution and sub-100 nm depth penetration, which enabled discrimination between amorphous and crystalline material. Whilst there are limited examples of this technique in characterising inhaled APIs, this approach may enable greater understanding of the distribution of process induced surface disorder in micronized API.

4. Chemical imaging

The combination of spectroscopy and microscopy has enhanced the ability to characterise the properties of pharmaceutical materials. Whist spectroscopic investigations yield chemical and physical information, microscopy provides both lateral and spatial resolution [115]. The development of these combination systems enables spatial focusing and rastering of the exciting radiation (e.g. Raman spectroscopy), or microscopy approaches that present physicochemical information from secondary signals.

Chemical imaging probes intrinsic properties of a molecule or atom, often in a non-invasive way. Spatially resolved chemical information provides valuable data, which maybe represented in a colour-coded distribution map of a system. The utilisation of chemical imaging enables investigation of visual appearance and chemical/physical state of a material. Typically, chemical imaging of MDI and DPI drug products has been used to identify ingredients present within the formulation, in addition, to particle size, morphology and shape. Furthermore, content uniformity, sample homogeneity and spatial distribution of components of inhaled dosage forms have been investigated using chemical imaging [116].

4.1 Energy-dispersive X-ray spectroscopy (EDX)

Energy-dispersive X-ray spectroscopy (EDX) is an analytical technique used in combination with SEM for the elemental analysis of a sample. The sampling depth of EDX is approximately 10 nm and is performed using X-rays emitted by the material in response to interacting with charged particles. As each

element has a unique atomic structure they produce characteristic X-rays, which allow an element's atomic structure to identified uniquely from one another [34]. SEM requires coating of the sample surface with a thin conducting layer of carbon, platinum or gold. Carbon is the coating material used for EDX, because it does not limit spectral resolution of EDX and does not disturb the emission of the X-ray signals of the sample.

Modern SEMs allow a spatial resolution down to a few nanometres. For EDX this resolution is difficult to achieve, which is related to limited acquisition times. In addition, an EDX map consists of a much lower number of pixels than a typical SEM image. As most API and excipients are organic materials, and therefore contain carbon, oxygen and hydrogen atoms, discrimination of components by EDX is difficult because no intrinsic marker is present. Hence, for substantial spatial discrimination of ingredients by EDX mapping, the presence of at least one component including a different element, e.g. sulphur, phosphorous or chlorine is required. If such an element is present in the API or any of the excipients, the distribution within the material can be characterized.

EDX has been utilised in the characterization of spray dried ipratropium bromide particles [117]. Corrigan *et al*., used EDX to show that following spray drying of ipratropium bromide from different ethanol solutions the material remained as a bromide salt.

4.2 Time-of-flight secondary ion mass spectroscopy (TOF-SIMS)

Time-of-flight secondary ion mass spectroscopy (TOF-SIMS) is another method employed for chemical imaging. It uses a focused, pulsed primary ion beam to produce secondary molecular ions from the surface monolayer of a sample [118]. The ejected secondary ions are collected and their mass is determined by measuring the exact time at which they reach the detector. It is possible to measure the time-of-flight on a scale of nano-seconds, which produces high mass resolution down to 0.001 atomic mass units (amu) at a range of typically 0–10.000 amu [119]. The limit of detection can be as low as part, per billion although TOF-SIMS generally does not allow fully quantitative analysis. The ion beam can be scanned over a sample to produce maps at sub-micrometre resolution. TOF-SIMS is a highly surface sensitive method being able to detect molecules within a depth of a few angstroms, and is useful to determine the elemental, isotopic or molecular composition of the surface [120]. TOF-SIMS is ideal for probing flat surfaces, however, microscopically rough surfaces maybe imaged. The charging of materials due to irradiating ions may also limit analysis of certain materials by TOF-SIMS, particularly those that are poorly conducting.

Blister packaging material used in DPIs have been characterised by ToF-SIMS [121]. Bunker *et al*., investigated two configurations of blisters that consisted of either two strips of polymer coated metal foil and the other had a series of pockets punched in a line. The two sides are glued together to hold the individual doses of powder in place in the pockets. ToF-SIMS confirmed

that materials have different surface chemistry. Furthermore, ToF-SIMS was able to show spatial mapping of the PVC and tin chloride when the two strips were formed together.

The ToF-SIMS has also been utilised in the mapping of lactose and lactose processed with magnesium stearate [122]. Zhou et al. found that spatial mapping of untreated lactose sample showed elements of carbon, hydrogen and oxygen, with no presence of magnesium. On processing lactose with magnesium stearate using mechanofusion, it was possible to detect magnesium at the surface of the powder materials.

4.3 Raman microscopy

Although automated image analysis offers significant practical advantage relative to manual microscopy, it shares the limitation of being unable to discriminate between API and excipient particles that are visually identical. Adding an additional analytical probe, for example, the addition of a Raman microprobe, can increase the potential of automated imaging.

Raman spectroscopy is based on the inelastic scattering of monochromatic light when the frequency of photons changes upon interaction with a sample, within a given sample depth [123]. The photons of the laser light are absorbed by the sample and subsequently reemitted. The frequency of the re-emitted photons is shifted up or down in comparison with the original monochromatic

frequency, and is known as the Raman effect [43]. The Raman shift provides information about vibrational and rotational energies of molecular bonds. It was realized that Raman spectroscopy was a convenient probe of the vibrational energy levels within a molecule, which easily provides molecular fingerprints [124]. Another unique advantage of Raman spectroscopy is it can be used to selectively analyse components of a material by changing the excitation wavelength. In addition, Raman spectroscopy does not require invasive sample preparation and Raman spectra usually contain sharp bands that are characteristic of the specific molecular bonds in the sample [15]. The intensity of the bands in a Raman spectrum is proportional to the concentration of the corresponding molecules and, thus, can be used for quantitative analysis of the surfaces of materials [125]. The key to robust Raman microscopy analysis of pharmaceutical materials is related to the spot size of the laser and therefore the optical resolution, which is diffraction limited. The optical resolution must be optimised for improved image quality.

There are an increasing number of publications that have utilised Raman microscopy to investigated inhaled pharmaceutical materials. For example, confocal Raman microscopy has been used by Ward *et al*., to identify and map surface amorphous domains on particles of sorbitol. They were able to use Raman mapping to distinguish crystalline and amorphous regions. The distinction was possible due to the shift in the vibrational bands, which were altered by the molecules physical environment. Confocal Raman microscopy revealed the distribution of amorphous sorbitol material within the thermally modified region. This type of experiment was not possible with AFM due to

the large vertical height differences across the sample. Using z-stacking, they were able to image the amorphous domain down to a depth of 20 nm. This profile qualitatively related to the heat transfer from the scanning thermal probe tip, which was used to generate the amorphous domain on the sorbitol surface.

Steele *et al*., demonstrated the use of scanning Raman microscopy to map aerosol particulate deposits produced from MDI [126]. They aerosolized commercially available combination asthma therapy MDI containing salbutamol and beclometasone dipropionate into an Andersen cascade impactor (ACI), and analyzed the deposition plated by conventional in vitro quantitative analysis and scanning Raman microscopy. Raman maps, taken from Andersen cascade impactor plate stages 3 and 5 (>100 μm^2 areas) showed good correlation with chemical analysis of the respective stages.

Another study has utilized Raman microscopy to investigate the co-deposition of salmeterol and fluticasone propionate by a commercially available combination MDI [127]. This combination based therapy shows greater efficacy compared with monotherapy treatments with the individual components, due to synergistic interactions of the two classes of compounds at the receptor, molecular and cellular level [128]. In order to investigate, the co-deposition profile of the two APIs, the MDI was aerosolized into an ACI, and the APIs deposited on stage 4 were investigated by Raman microscopy. In this study, Theophilus *et al.*, used the Jaccard coefficient to measure the co-association of the two drugs upon deposition in the ACI, which was

computed from the statistically threshold Raman images. Furthermore, the statistical validity of the co-deposition of the two drugs was determined using the bootstrapping technique. In this way, it was found significant co-association of salmeterol and fluticasone propionate, leading to increased co-deposition. A similar finding was also found by Rogueda *et al*., who found using Raman microscopy that the fluticasone and salmeterol agglomerated more extensively than budesonide and formoterol upon aerosolization into an ACI. In this study, AFM measurements also confirmed greater chemical affinity between fluticasone and salmeterol in comparison to budesonide and formoterol [92]. It was thought this occurrence provided greater opportunity for synergistic interaction between the two drugs in the airways upon aerosolization.

Raman chemical imaging has much potential for the investigation of DPI formulations. Since DPI dosage forms are complex, the ability to chemically identify components of the formulation may enable greater investigation into the structure of the formulation. An example, of bright-field reflectance and Raman chemical image of fluticasone propionate and lactose, collected on stage 3 of a next generation impactor (NGI) following aerosolization of an Advair DPI (500/50) is shown in Fig. 8. These data were collected using a ChemImage Falcon II Raman imaging system (Pittsburgh, USA). In addition, the particle size of each component on stage 3 was determined. These data showed that lactose and fluticasone were delivered independent of each other. In addition, the volume-weighted median diameter of the API was larger than that of the lactose.

Recently, Sasic and Harding investigated combination DPI formulations using global illumination Raman chemical imaging [129]. In this study, two APIs were mixed with carrier lactose particles using a Diosna high shear mixer. Raman chemical imaging enabled imaging of APIs adhered to the surface of large particles of lactose or as agglomerates on the lactose surface. Furthermore, mechanical and light dispersion method for dispersing particles for imaging was investigated. The method of dispersion was found to have a profound effect on the API deposits because the mechanical dispersion leads to complete separation of lactose and API particles previously adhered to its surface. These results suggested a significant potential of this imaging technique for fast and reliable visualization of DPI formulations.

Raman chemical imaging and scanning electron microscopy (Raman/SEM) have been used in a preliminary study to determine the size, morphology, elemental and molecular composition, and molecular structure of fine particulate matter in several test samples and one ambient air sample. Raman chemical imaging and SEM, respectively, provide a way to spatially characterize a sample based on its molecular and elemental makeup. When combined, Raman chemical imaging and SEM provide detailed spatial, elemental, and molecular information for particulate matter as small as 250nm. Initial studies demonstrate the potential of Raman/SEM for molecular and elemental determination of organic and inorganic fine particulate matter [130]. This has been accomplished by analyzing samples with fine particulate

matter using each method independently. Since both techniques are nondestructive, particles of interest can be relocated between instruments.

Scanning electron microscopy (SEM) is a useful tool to examine drug formulations. If low vacuum scanning electron microscopy is used then un-coated sections can be imaged using backscattered electrons – these yield atomic number contrast, which is useful for distinguishing between phases that might appear similar optically. In combination with Raman spectroscopy can be used to analyse their chemistry. Renishaw's SEM is a standard tungsten-filament model (JEOL JSM-6060LV) capable of low vacuum operation, and fitted with a dual-channel (VIS/NIR) SEM-SCA.

This system has recently been utilised by Shur and Price in the investigation of the distribution of budesonide and formoterol within carrier based DPI formulations [130]. Their investigations suggested the presence of separate budesonide only and formoterol only agglomerates on the lactose surface, while there is little or no interaction of BUD to FFD and vice versa. This system shows great promise in the investigation of the formulation microstructure of carrier based DPI formulations.

5. Application of Tomography Image Analysis

It is of significant interest to determine the structural features of OIDP formulations. One drawback of some of the techniques is that their invasive nature can destroy the sample and prevent any further testing. Another is the

techniques' limited penetration and resolution. Thus, it is probably fair to say that the ideal experimental approach for the three-dimensional structural imaging of pharmaceutical dosage forms has not yet been realized.

X-ray microtomography is a relatively new approach to imaging the internal structure of solid dosage forms. This technique has been widely used for the in vivo imaging of plants, insects, animals, and humans. X-ray microtomography is a non-destructive technique that has high penetration ability and provides a reasonable level of resolution (~5–20 μm) [131].

The X-ray microtomography utilises X-rays that are directed from a high-power source toward a sample, and a detector on the opposite side of the sample measures the intensity of the transmitted X-rays. A two-dimensional "shadow" image is produced by accurately rastering the X-ray beam across the sample. The sample then is carefully moved (usually rotated) relative to the X-ray beam, and the process is repeated to produce additional two-dimensional images from various view points [132]. Using a sophisticated Fourier transform algorithm, the two-dimensional images then are combined to generate a complete three-dimensional map of the sample. In very simple terms, X-ray microtomography can be thought of as creating a three-dimensional map of the relative atomic density of the sample under evaluation.

X-ray microtomography is being utilised to investigate pharmaceutical materials, however, there are limited examples in the literature with regards to

their application for characterizing OIDPs. This technique has, however, been utilised by valve manufactures to assess the crimping of valves to MDI cans and in assessing the leakage potential with certain valve and can combinations [133]. A study by Miller and Dey used X-ray microtomography to make non-destructive density measurements in compacted lactose powder samples [134]. In a recent study, X-ray microtomography has been utilised in the development of inhaler hardware during development [135]. The capability of this technique to form 3D constructions of the sample interest, may afford the opportunity to investigate the structure of DPI formulations in greater detail.

6. Future Directions

As the role of surface and interfacial properties of materials are critically important to the processing, structure and functionality of OIDPs, the identification and measurement of their critical quality attributes has become the key area for OIDP development. The need to implement a Quality by Design (QbD) approach during product development and manufacturing of OIDPs, will manoeuvre the chemistry, manufacturing and controls (CMC) of excipients and APIs towards a greater understanding of their impact on product quality. Identifying these parameters requires greater implementation of physical and chemical analyses at the microscopic level. With the continuing development of scanning microscopes and their coupling with spectroscopic techniques, greater understanding of these critical quality

attributes may enhance our control, handling and processing of particulate matter for the development of OIDPs.

6. References

[1] H.D. Smyth, Propellant-driven metered-dose inhalers for pulmonary drug delivery, Expert Opin. Drug Deliv. 2 (2005) pp. 53–74.

[2] S.P. Newman, Principles of metered-dose inhaler design, Respir. Care. 50 (2005) pp. 1177–1190.

[3] K.J. McDonald, G.P. Martin, Transition to CFC-free metered dose inhalers--into the new millennium, Int. J. Pharm. 201 (2000) pp. 89–107.

[4] M.J. Telko, A.J. Hickey, Dry powder inhaler formulation, Respir. Care. 50 (2005) pp. 1209–1227.

[5] S. Edge, S. Mueller, R. Price, J. Shur, Factors affecting defining the quality and functionality of excipients used in the manufacture of dry powder inhaler products, Drug Dev. Ind. Pharm. 34 (2008) pp. 966–973.

[6] H.-K. Chan, Dry powder aerosol drug delivery - Opportunities for colloid and surface scientists, Colloid Surface A. 284 (2006) pp. 50–55.

[7] T. Srichana, G. Martin, C. Marriott, On the relationship between drug and carrier deposition from dry powder inhalers in vitro, Int. J. Pharm. 167 (1998) pp.13–23.

[8] P. Rogueda, Novel hydrofluoroalkane suspension formulations for respiratory drug delivery, Expert Opin. Drug Deliv. 2 (2005) pp. 625–638.

[9] S. Newman, Evolution of dry powder inhaler design, formulation, and performance, Respir. Med. 96 (2002) pp. 293–304.

[10] A.J. Hickey, H.M. Mansour, M.J. Telko, Z. Xu, H.D.C. Smyth, T. Mulder, R. McLean, J. Langridge, D. Papadopoulos, Physical characterization of component particles included in dry powder inhalers. I. Strategy review and static characteristics, J. Pharm. Sci. 96 (2007) pp. 1282–1301.

[11] V. Lehto, T. Lankinen, Moisture transfer into medicament chambers equipped with a double-barrier-desiccant system, Int. J. Pharm. 275 (2004) pp.155–164.

[12] W.K. Ng, J.W. Kwek, R.B.H. Tan, Anomalous particle size shift during post-milling storage, Pharm. Res. 25 (2008) pp. 1175–1185.

[13] United States Pharmacopoeia, (31st Rev. ed.), Aerosol <601> (2008). Rockville, MD: The United States Pharmacopoeial Convention, Inc, Retrieved September 8, 2008, from www.uspnf.com.

[14] Food and Drug Administration, Guidance for Industry Metered dose inhaler (MDI) and dry powder inhaler (DPI) drug products. Chemistry, manufacturing and controls, (1998), Retrieved September 8, 2008, from www.fda.gov.

[15] P. Cooke, Chemical microscopy, Anal. Chem. 72 (2000) pp.169R–188R.

[16] S. Surman, J. Walker, D. Goddard, L. Morton, C. Keevil, W. Weaver, et al., Comparison of microscope techniques for the examination of biofilms, J. Microbiol. Meth. 25 (1996) pp. 57–70.

[17] B. Ruozi, D. Belletti, A. Tombesi, G. Tosi, L. Bondioli, F. Forni, M.A. Vandelli, AFM, ESEM, TEM, and CLSM in liposomal characterization: a comparative study, Int. J. Nanomed. 6 (2011) pp. 557–563.

[18] P.M. Young, R. Price, M.J. Tobyn, M. Buttrum, F. Dey, Effect of humidity on aerosolization of micronized drugs., Drug Dev. Ind Pharm. 29 (2003) pp. 959–966.

[19] N. Islam, P. Stewart, I. Larson, P. Hartley, Lactose surface modification by decantation: are drug-fine lactose ratios the key to better dispersion of salmeterol xinafoate from lactose-interactive mixtures?, Pharm. Res. 21 (2004) pp. 492–499.

[20] M. Bunker, M. Davies, C. Roberts, Towards screening of inhalation formulations: measuring interactions with atomic force microscopy, Expert Opin. Drug Deliv. 2 (2005) pp. 613–624.

[21] M. Davies, A. Brindley, X. Chen, M. Marlow, S. Doughty, I. Shrubb, C.J. Roberts, Characterization of drug particle surface energetics and Young's modulus by atomic force microscopy and inverse gas chromatography, Pharm. Res. 22 (2005) pp. 1158–1166.

[22] D. Traini, P. Rogueda, P. Young, R. Price, Surface Energy and Interparticle Force Correlation in Model pMDI Formulations, Pharm. Res. 22 (2005) pp. 816–825.

[23] X. Liao, T. Wiedmann, Characterization of pharmaceutical solids by scanning probe microscopy, J. Pharm. Sci. 93 (2004) pp. 2250–2258.

[24] D. Shotton, Electronic Light-Microscopy - Present Capabilities and Future-Prospects, Histochem. Cell Biol. 104 (1995) pp. 97–137.

[25] A.S. Elkady, Scanning transmitted and reflected light microscopy: A novel microscopy for visualizing biomaterials at interfaces, Micron. 38 (2007) pp. 848–853.

[26] J. Mitchell, S. Newman, H.-K. Chan, In vitro and in vivo aspects of cascade impactor tests and inhaler performance: a review, AAPS Pharm. Sci. Tech. 8 (2007) pp. E1-E12.

[27] United States Pharmacopoeia, (31st Rev. ed.), Particulate matter in injections <788> (2008). Rockville, MD: The United States Pharmacopoeial Convention, Inc, Retrieved September 8, 2008, from www.uspnf.com.

[28] P. O'Shaughnessy, M. Barsotti, J. Fay, S. Tighe, Evaluating particle counters, J. Am. Water Works Ass. 89 (1997) pp. 60–70.

[29] M. Niemann, M. Fusser, L. Scaffidi, A critical comparison: Particle counting with light obscuration and automated Raman microscopy, in: R.N. Dalby, P.R. Byron, J. Peart, J.D. Suman and S.J. Farr, Respiratory Drug Delivery X, Boca Raton, USA, 2006, pp. 529–532.

[30] H. Larhrib, G. Martin, C. Marriott, D. Prime, The influence of carrier and drug morphology on drug delivery from dry powder formulations, Int. J. Pharm. 257 (2003) pp. 283–296.

[31] W. Kaialy, G.P. Martin, M.D. Ticehurst, P. Royall, M.A. Mohammad, J. Murphy, et al., Characterisation and deposition studies of recrystallised lactose from binary mixtures of ethanol/butanol for improved drug delivery from dry powder inhalers, AAPS J. 13 (2011) pp. 30–43.

[32] W. Kaialy, M.N. Momin, M.D. Ticehurst, J. Murphy, A. Nokhodchi, Engineered mannitol as an alternative carrier to enhance deep lung penetration of salbutamol sulphate from dry powder inhaler, Colloids Surf, B. 79 (2010) pp. 345–356.

[33] R. Oldenbourg, Polarized light field microscopy: an analytical method using a microlens array to simultaneously capture both conoscopic and orthoscopic views of birefringent objects, J. Microsc. (Oxf). 231 (2008) pp. 419–432.

[34] K. Knowles, F. Freeman, Microscopy and microanalysis of crystalline glazes, J. Microsc. (Oxf). 215 (2004) pp. 257–270.

[35] Y. Omura, R. Okamoto, M. Konno, M. Shiro, Problems in polarized light microscopy observation of birefringence of calcium pyrophosphate dihydrate crystals, Micron. 41 (2010) pp. 974–982.

[36] R. Price, P.M. Young, Visualization of the crystallization of lactose

from the amorphous state, J. Pharm. Sci. 93 (2003) pp. 155–164.

[37] J. Shur, T.G. Nevell, R.J. Ewen, R. Price, A. Smith, E. Barbu, J.H. Conway, M.P. Carroll, J.K. Shute, J.R. Smith, Cospray-dried unfractionated heparin with L-leucine as a dry powder inhaler mucolytic for cystic fibrosis therapy, J. Pharm. Sci. 97 (2008) pp. 4857–4868.

[38] S.A.E. Boyer, J.M. Haudin, Crystallization of polymers at constant and high cooling rates: A new hot-stage microscopy set-up, Polym. Test. 29 (2010) pp. 445–452.

[39] I. Vitez, A. Newman, M. Davidovich, C. Kiesnowski, The evolution of hot-stage microscopy to aid solid-state characterizations of pharmaceutical solids, Thermochim. Acta. 327 (1998) pp. 187–196.

[40] H. Chan, I. Gonda, Solid state characterization of spray-dried powders of recombinant human deoxyribonuclease (RhDNase), J. Pharm. Sci. 87 (1998) pp. 647–654.

[41] E.M. Littringer, A. Mescher, S.G. Maas, P. Walzel, N.A. Urbanetz, Influence of droplet size on the crystallization behaviour of aqueous D-mannitol solutions during spray drying, in: 24th European Conference on Liquid Atomization and Spray Systems, Estoril, Portugal, 2011, pp. 1–8.

[42] X. Sun, L. Tolbert, J. Hildebrand, Using Laser-Scanning Confocal Microscopy as a Guide for Electron-Microscopic Study - a Simple Method for Correlation of Light and Electron-Microscopy, J. Histochem. Cytochem. 43 (1995) pp. 329–335.

[43] C. Maggiano, T. Dupras, M. Schultz, J. Biggerstaff, Confocal laser scanning microscopy: a flexible tool for simultaneous polarization and three-dimensional fluorescence imaging of archaeological compact bone, J. Archaeol. Sci. 36 (2009) pp. 2392–2401.

[44] N.Y. Chew, H.K. Chan, Use of solid corrugated particles to enhance powder aerosol performance, Pharm. Res. 18 (2001) pp. 1570–1577.

[45] S.G. Maas, G. Schaldach, E.M. Littringer, A. Mescher, U.J. Griesser, D.E. Braun, et al., The impact of spray drying outlet temperature on the particle morphology of mannitol, Powder Technology. 213 (2011) pp. 27–35.

[46] G. Casuccio, S. Schlaegle, T. Lersch, G. Huffman, Y. Chen, N. Shah, Measurement of fine particulate matter using electron microscopy techniques, Fuel Process Technol. 85 (2004) pp. 763–779.

[47] C. Srinivasan, T.J. Mullen, J.N. Hohman, M.E. Anderson, A.A. Dameron, A.M. Andrews, E.C. Dickey, M.W. Horn, P.S. Weiss, Scanning electron microscopy of nanoscale chemical patterns, ACS Nano. 1 (2007) pp. 191–201.

[48] V. Berard, E. Lesniewska, C. Andres, D. Pertuy, C. Laroche, Y. Pourcelot, Dry powder inhaler: influence of humidity on topology and adhesion studied by AFM, Int. J. Pharm. 232 (2002) pp. 213–224.

[49] M. Murtomaa, V. Mellin, P. Harjunen, T. Lankinen, E. Laine, V. Lehto, Effect of particle morphology on the triboelectrification in dry powder inhalers, Int. J. Pharm. 282 (2004) pp. 107–114.

[50] J. Shur, T.G. Nevell, J.K. Shute, J.R. Smith, The spray drying of unfractionated heparin: optimization of the operating parameters., Drug Dev. Ind. Pharm. 34 (2008) pp. 559–568.

[51] Y. Maa, P. Nguyen, T. Sweeney, S. Shire, C. Hsu, Protein inhalation powders: Spray drying vs spray freeze drying, Pharm. Res. 16 (1999) pp. 249–254.

[52] B. Shekunov, J. Feeley, A. Chow, H. Tong, P. York, Aerosolisation behaviour of micronised and supercritically-processed powders, J. Aerosol Sci. 34 (2003) pp. 553–568.

[53] J. Kaerger, R. Price, Processing of spherical crystalline particles via a novel solution atomization and crystallization by sonication (SAXS) technique, Pharm. Res. 21 (2004) pp. 372–381.

[54] D. Murnane, C. Marriott, G.P. Martin, In situ and Ex situ analysis of salmeterol xinafoate microcrystal formation from poly(ethylene glycol) 400 - Water cosolvent mixtures, Cryst. Growth. Des. 8 (2008) pp.1855–1862.

[55] H. Adi, D. Traini, H.-K. Chan, P.M. Young, The influence of drug morphology on aerosolisation efficiency of dry powder inhaler formulations, J. Pharm. Sci. 97 (2008) pp. 2780–2788.

[56] C. Pitchayajittipong, R. Price, J. Shur, J.S. Kaerger, S. Edge, Characterisation and functionality of inhalation anhydrous lactose, Int. J. Pharm. 390 (2010) pp. 134–141.

[57] Y. Kawashima, T. Serigano, T. Hino, H. Yamamoto, H. Takeuchi, Effect of surface morphology of carrier lactose on dry powder inhalation property of pranlukast hydrate, Int. J. Pharm. 172 (1998) pp. 179–188.

[58] X. Zeng, G. Martin, C. Marriott, J. Pritchard, Lactose as a carrier in dry powder formulations: The influence of surface characteristics on drug delivery, J. Pharm. Sci. 90 (2001) pp.1424–1434.

[59] P. Heng, L. Chan, L. Lim, Quantification of the surface morphologies of lactose carriers and their effect on the in vitro deposition of salbutamol sulphate, Chem. Pharm. Bull. 48 (2000) pp. 393–398.

[60] Z. Xu, H.M. Mansour, T. Mulder, R. McLean, J. Langridge, A.J. Hickey, Dry powder aerosols generated by standardized entrainment tubes from drug blends with lactose monohydrate: 2. Ipratropium bromide monohydrate and fluticasone propionate, J. Pharm. Sci. 99 (2010) pp. 3415–3429.

[61] P.M. Young, P. Kwok, H. Adi, H.-K. Chan, D. Traini, Lactose Composite Carriers for Respiratory Delivery, Pharm. Res. 26 (2008) pp. 802–810.

[62] M.J. Donovan, H.D.C. Smyth, Influence of size and surface roughness of large lactose carrier particles in dry powder inhaler formulations, Int. J. Pharm. 402 (2010) pp. 1–9.

[63] F. Ferrari, D. Cocconi, R. Bettini, F. Giordano, P. Santi, M. Tobyn, R. Price, P.M. Young, C. Caramella, P. Colombo, The surface roughness of lactose particles can be modulated by wet-smoothing using a high-shear mixer, AAPS Pharm. Sci. Tech. 5 (2004) pp. 1–6.

[64] P.M. Young, H.-K. Chan, H. Chiou, S. Edge, T.H.S. Tee, D. Traini, The influence of mechanical processing of dry powder inhaler carriers on drug aerosolization performance, J. Pharm. Sci. 96 (2007) pp. 1331–1341.

[65] J. Shur, H. Harris, M.D. Jones, J.S. Kaerger, R. Price, The role of fines in the modification of the fluidization and dispersion mechanism within dry powder inhaler formulations, Pharm. Res. 25 (2008) pp. 1631–1640.

[66] M.D. Jones, H. Harris, J.C. Hooton, J. Shur, G.S. King, C.A. Mathoulin, K. Nichol, T.L. Smith, M.L. Dawson, A.R. Ferrie, R. Price, An investigation into the relationship between carrier-based dry powder inhalation performance and formulation cohesive-adhesive force balances., Eur. J. Pharm. Biopharm. 69 (2008) pp. 496–507.

[67] M.D. Jones, R. Price, The Influence of Fine Excipient Particles on the Performance of Carrier-Based Dry Powder Inhalation Formulations, Pharm. Res. 23 (2006) pp. 1665–1674.

[68] H. Adi, I. Larson, H. Chiou, P. Young, D. Traini, P. Stewart, Agglomerate Strength and Dispersion of Salmeterol Xinafoate from Powder Mixtures for Inhalation, Pharm. Res. 23 (2006) pp. 2556–2565.

[69] S.E. Kirk, J.N. Skepper, A.M. Donald, Application of environmental

scanning electron microscopy to determine biological surface structure, J Microsc. (Oxf). 233 (2009) pp. 205–224.

[70] S. Wight, C. Zeissler, Environmental Scanning Electron-Microscope Imaging Examples Related to Particle Analysis, Microsc. Res. Techniq. 25 (1993) pp. 393–397.

[71] C.P. Watling, J.A. Elliott, C. Scruton, R.E. Cameron, Surface modification of lactose inhalation blends by moisture, Int. J. Pharm. 391 (2010) pp. 29–37.

[72] G. Huyang, J. Canning, B.C. Gibson, T. Khoury, T.J. Sum, C. Neto, M.J. Crossely, Focused ion beam processing and engineering of devices in self-assembled supramolecular structures, Nanotechnology. 20 (2009) pp. 1-6.

[73] A. Friedmann, A. Hoess, A. Cismak, A. Heilmann, Investigation of cell-substrate interactions by focused ion beam preparation and scanning electron microscopy, Acta Biomater. 7 (2011) pp. 2499–2507.

[74] P.K. Wallace, B. Arey, W.F. Mahaffee, Subsurface examination of a foliar biofilm using scanning electron- and focused-ion-beam microscopy, Micron. 42 (2011) 579–585.

[75] D. Heng, P. Tang, J.M. Cairney, H.-K. Chan, D.J. Cutler, R. Salama, et al., Focused-ion-beam milling: A novel approach to probing the interior of particles used for inhalation aerosols, Pharm. Res. 24 (2007) pp. 1608–1617.

[76] N. Chew, H. Chan, Influence of particle size, air flow, and inhaler device on the dispersion of mannitol powders as aerosols, Pharm. Res. 16 (1999) pp. 1098–1103.

[77] H.G. Hansma, L. Pietrasanta, Atomic force microscopy and other scanning probe microscopies, Curr. Opin. Chem. Biol. 2 (1998) pp. 579–584.

[78] G. Binnig, C. Quate, C. Gerber, Atomic force microscope, Phys. Rev. Lett. 56 (1986) pp. 930–933.

[79] H.G. Hansma, L.I. Pietrasanta, I.D. Auerbach, C. Sorenson, R. Golan, P.A. Holden, Probing biopolymers with the atomic force microscope: a review, J. Biomater. Sci. Polym. Ed. 11 (2000) pp. 675–683.

[80] F. Giessibl, Advances in atomic force microscopy, Rev. Mod. Phys. 75 (2003) pp. 949–983.

[81] M. Louey, P. Mulvaney, P.J. Stewart, Characterisation of adhesional

properties of lactose carriers using atomic force microscopy, Journal of Pharmaceutical and Biomedical Analysis. 25 (2001) pp. 559–567.

[82] R. Price, P.M. Young, S. Edge, J.N. Staniforth, The influence of relative humidity on particulate interactions in carrier-based dry powder inhaler formulations, Int. J. Pharm. 246 (2002) pp. 47–59.

[83] C.J. Roberts, What can we learn from atomic force microscopy adhesion measurements with single drug particles?, Eur. J. Pharm. Sci. 24 (2005) pp.153–157.

[84] N. Islam, P. Stewart, I. Larson, P. Hartley, Surface roughness contribution to the adhesion force distribution of salmeterol xinafoate on lactose carriers by atomic force microscopy, J. Pharm. Sci. 94 (2005) pp.1500–1511.

[85] S.C. Strathmann, M.A. Murphy, B.A. Goeckner, P.W. Carter, J.-B.D. Green, Forces between insulin microspheres and polymers surfaces for a dry powder inhaler, Int. J. Pharm. 372 (2009) pp.147–153.

[86] P.M. Young, R. Price, The influence of humidity on the aerosolisation of micronised and SEDS produced salbutamol sulphate, Eur. J. Pharm. Sci. 22 (2004) pp. 235–240.

[87] M.D. Louey, P.J. Stewart, Particle interactions involved in aerosol dispersion of ternary interactive mixtures., Pharm. Res. 19 (2002) pp. 1524–1531.

[88] P.M. Young, R. Price, D. Lewis, S. Edge, D. Traini, Under pressure: predicting pressurized metered dose inhaler interactions using the atomic force microscope, J. Colloid. Interf. Sci. 262 (2003) pp. 298–302.

[89] D. Traini, P. Rogueda, P. Young, R. Price, Surface energy and interparticle force correlation in model pMDI formulations, Pharm. Res. 22 (2005) pp. 816–825.

[90] D. Traini, P.M. Young, P. Rogueda, R. Price, In Vitro investigation of drug particulates interactions and aerosol performance of pressurised metered dose Inhalers, Pharm. Res. 24 (2006) pp. 125–135.

[91] P.M. Young, H. Adi, T. Patel, K. Law, P. Rogueda, D. Traini, The influence of micronised particulates on the aerosolisation properties of pressurised metered dose inhalers, J. Aerosol Sci. 40 (2009) pp. 324–337.

[92] P.G.A. Rogueda, R. Price, T. Smith, P.M. Young, D. Traini, Particle synergy and aerosol performance in non-aqueous liquid of two combinations metered dose inhalation formulations: An AFM and

Raman investigation, J. Colloid. Interf. Sci. 361 (2011) pp. 649–655.

[93] M. Esayanur, S. Yeruva, Y. Rabinovich, B. Moudgil, Interaction force measurements using atomic force microscopy for characterization and control of adhesion, dispersion and lubrication in particulate systems, J. Adhes. Sci. Technol. 19 (2005) pp. 611–626.

[94] Y.T.A. Turner, C.J. Roberts, M.C. Davies, Scanning probe microscopy in the field of drug delivery, Adv. Drug Deliv. Rev. 59 (2007) pp. 1453–1473.

[95] J.C. Hooton, C.S. German, S. Allen, M.C. Davies, C.J. Roberts, S.J.B. Tendler, P.M. Williams, Characterization of particle-interactions by atomic force microscopy: effect of contact area, Pharm. Res. 20 (2003) pp. 508–514.

[96] J.C. Hooton, C.S. German, S. Allen, M.C. Davies, C.J. Roberts, S.J.B. Tendler, P.M. Williams, An Atomic Force Microscopy Study of the Effect of Nanoscale Contact Geometry and Surface Chemistry on the Adhesion of Pharmaceutical Particles, Pharm. Res. 21 (2004) pp. 953–961.

[97] P. Begat, D. Morton, J. Staniforth, R. Price, The cohesive-adhesive balances in dry powder inhaler formulations I: Direct quantification by atomic force microscopy, Pharm. Res. 21 (2004) pp. 1591–1597.

[98] P. Begat, D. Morton, J. Staniforth, R. Price, The cohesive-adhesive balances in dry powder inhaler formulations II: Influence on fine particle delivery characteristics, Pharm. Res. 21 (2004) pp.1826–1833.

[99] J.C. Hooton, M.D. Jones, R. Price, Predicting the behavior of novel sugar carriers for dry powder inhaler formulations via the use of a cohesive-adhesive force balance approach, J. Pharm. Sci. 95 (2006) pp. 1288–1297.

[100] J.C. Hooton, M.D. Jones, H. Harris, J. Shur, R. Price, The influence of crystal habit on the prediction of dry powder inhalation formulation performance using the cohesive-adhesive force balance approach, Drug. Dev. Ind. Pharm. 34 (2008) pp. 974–983.

[101] M.D. Jones, J.C. Hooton, M.L. Dawson, A.R. Ferrie, R. Price, An Investigation into the dispersion mechanisms of ternary dry powder inhaler formulations by the quantification of interparticulate forces, Pharm. Res. 25 (2007) pp. 337–348.

[102] J. Shur, J.S. Kaerger, R. Price, Effect of surface amorphous content of active pharmaceutical ingredients on the performance of dry powder inhaler formulations, in: R.N. Dalby, P.R. Byron, J. Peart and J.D. Suman, Respiratory Drug Delivery 2007, Paris, France, 2007,

pp. 341–344.

[103] S. Morita, S. Fujisawa, E. Kishi, M. Ohta, H. Ueyama, Y. Sugawara, Contact and non-contact mode imaging by atomic force microscopy, Thin Solid Films. 273 (1996) pp. 138–142.

[104] P. Begat, P. Young, S. Edge, J. Kaerger, R. Price, The effect of mechanical processing on surface stability of pharmaceutical powders: Visualization by atomic force microscopy, J. Pharm. Sci. 92 (2003) pp. 611–620.

[105] D. Traini, P. Young, M. Jones, S. Edge, R. Price, Comparative study of erythritol and lactose monohydrate as carriers for inhalation: Atomic force microscopy and in vitro correlation, Eur. J. Pharm. Sci. 27 (2006) pp. 243–251.

[106] M. Jones, J. Hooton, M. Dawson, A. Ferrie, R. Price, Dehydration of trehalose dihydrate at low relative humidity and ambient temperature, Int. J. Pharm. 313 (2006) pp. 87–98.

[107] P.M. Young, D. Cocconi, P. Colombo, R. Bettini, R. Price, D.F. Steele, M.J. Tobyn, Characterization of a surface modified dry powder inhalation carrier prepared by “particle smoothing,” J. Pharm. Pharmacol. 54 (2002) pp. 1339–1344.

[108] A. Danesh, X. Chen, M. Davies, C. Roberts, G. Sanders, S. Tendler, et al., Polymorphic discrimination using atomic force microscopy: Distinguishing between two polymorphs of the drug cimetidine, Langmuir. 16 (2000) pp. 866–870.

[109] A. Baker, M. Miles, W. Helbert, Internal structure of the starch granule revealed by AFM, Carbohydr. Res. 330 (2001) pp. 249–256.

[110] R. Price, P. Young, On the physical transformations of processed pharmaceutical solids, Micron. 36 (2005) pp. 519–524.

[111] B. Bowe, V. Toal, White light interferometric surface profiler, Opt. Eng. 37 (1998) pp. 1796–1799.

[112] S. Adi, H. Adi, H.-K. Chan, P.M. Young, D. Traini, R. Yang, A. Yu, Scanning white-light interferometry as a novel technique to quantify the surface roughness of micron-sized particles for inhalation, Langmuir. 24 (2008) pp. 11307–11312.

[113] L. Harding, J. Wood, M. Reading, D.Q.M. Craig, Two- and three-dimensional imaging of multicomponent systems using scanning thermal microscopy and localized thermomechanical analysis, Anal. Chem. 79 (2007) pp. 129–139.

[114] L. Harding, W.P. King, X. Dai, D.Q.M. Craig, M. Reading, Nanoscale

characterisation and imaging of partially amorphous materials using local thermomechanical analysis and heated tip AFM, Pharm. Res. 24 (2007) pp. 2048–2054.

[115] U. Schmidt, W. Ibach, J. Mueller, K. Weishaupt, O. Hollricher, Raman spectral imaging - A nondestructive, high resolution analysis technique for local stress measurements in silicon, Vib. Spectrosc. 42 (2006) pp. 93–97.

[116] H.M. Mansour, A.J. Hickey, Raman characterization and chemical imaging of biocolloidal self-assemblies, drug delivery systems, and pulmonary inhalation aerosols: a review, AAPS Pharm. Sci. Tech. 8 (2007) pp. E1-E16.

[117] D.O. Corrigan, O.I. Corrigan, A.M. Healy, Physicochemical and in vitro deposition properties of salbutamol sulphate/ipratropium bromide and salbutamol sulphate/excipient spray dried mixtures for use in dry powder inhalers, Int. J. Pharm. 322 (2006) pp. 22–30.

[118] S. Rabbani, A.M. Barber, J.S. Fletcher, N.P. Lockyer, J.C. Vickerman, TOF-SIMS with argon gas cluster ion beams: a comparison with C60+, Anal. Chem. 83 (2011) pp. 3793–3800.

[119] R. Ogaki, I.S. Gilmore, M.R. Alexander, F.M. Green, M.C. Davies, J.L.S. Lee, Surface mass spectrometry of two component drug-polymer systems: novel chromatographic separation method using gentle-secondary ion mass spectrometry (G-SIMS), Anal. Chem. 83 (2011) pp. 3627–3631.

[120] A.-C. Almstrand, M. Josefson, A. Bredberg, J. Lausmaa, P. Sjövall, P. Larsson, A-C. Olin, TOF-SIMS analysis of exhaled particles from patients with asthma and healthy controls., Eur. Respir. J. (2011) In Press.

[121] M.J. Bunker, M.C. Davies, X. Chen, M.B. James, C.J. Roberts, Single particle friction on blister packaging materials used in dry powder inhalers, Eur. J. Pharm. Sci. 29 (2006) pp. 405–413.

[122] Q.T. Zhou, L. Qu, T. Gengenbach, J.A. Denman, I. Larson, P.J. Stewart, D.A.V. Morton, Investigation of the extent of surface coating via mechanofusion with varying additive levels and the influences on bulk powder flow properties, Int. J. Pharm. 413 (2011) pp. 36–43.

[123] A. Kudelski, Raman spectroscopy of surfaces, Surf. Sci. 603 (2009) pp. 1328–1334.

[124] C. Schoenherr, T. Haefele, K. Paulus, G. Francese, Confocal Raman microscopy to probe content uniformity of a lipid based powder for inhalation: A quality by design approach, Eur. J. Pharm. Sci. 38 (2009) pp. 47–54.

[125] R.M. Connatser, S.M. Prokes, O.J. Glembocki, R.L. Schuler, C.W. Gardner, S.A. Lewis, L.A. Lewis, Toward surface-enhanced Raman imaging of latent fingerprints, J. Forensic Sci. 55 (2010) pp. 1462–1470.

[126] D.F. Steele, P.M. Young, R. Price, T. Smith, S. Edge, D. Lewis, The potential use of raman mapping to investigate in vitro deposition of combination pressurized metered-dose inhalers, AAPS Pharm. Sci. Tech. 6 (2004) pp. 1-4.

[127] A. Theophilus, A. Moore, D. Prime, S. Rossomanno, B. Whitcher, H. Chrystyn, Co-deposition of salmeterol and fluticasone propionate by a combination inhaler, Int. J. Pharm. 313 (2006) pp. 14–22.

[128] P.J. Barnes, Scientific rationale for inhaled combination therapy with long-acting 2-agonists and corticosteroids, European Respiratory Journal. 19 (2002) pp. 182–191.

[129] S. Šašić, L. Harding, Global illumination Raman chemical imaging of a combination of two drug molecules in a dry powder inhaler formulation, Anal. Methods. 2 (2010) pp.1528-1535.

[130] J. Shur, R. Price, Investigating the Structure-Function Relationship of Combination Dry Powder Inhaler Formulations, in: R.N. Dalby, P.R. Byron, J. Peart, J.D. Suman and P.M. Young, Respiratory Drug Delivery 2011, Berlin, Germany, 2011, pp. 479–482.

[131] X. Fu, M. Dutt, A.C. Bentham, B.C. Hancock, R.E. Cameron, J.A. Elliott, Investigation of particle packing in model pharmaceutical powders using X-ray microtomography and discrete element method, Powder Tech. 167 (2006) pp. 134–140.

[132] A.M. Miguélez-Morán, C.-Y. Wu, H. Dong, J.P.K. Seville, Characterisation of density distributions in roller-compacted ribbons using micro-indentation and X-ray micro-computed tomography, Eur. J. Pharm. Biopharm. 72 (2009) pp. 173–182.

[133] G. Williams, Computational X-Ray Tomography Techniques as Development Tools for Nasal and Pulmonary Device Optimization, in: R.N. Dalby, P.R. Byron, J. Peart, J.D. Suman and P.M. Young, Respiratory Drug Delivery 2010, Orlando, USA, 2010, pp. 895–898.

[134] N. Miller, F. Dey, Non-destructive density measurements of compacted lactose using X-ray microtomography, in: Drug Delivery to the Lungs 16, Edinburgh, UK, 2005, pp.18–22.

[135] A. Stuart, D. Clarke, The Role of X-Ray Computed Tomography as an Investigation Tool in Hardware Design, in: R.N. Dalby, P.R. Byron, J. Peart, J.D. Suman and P.M. Young, Respiratory Drug

Delivery 2009, Lisbon, Portugal, 2009, pp. 213–216.

Figures

Figure 1. Light microscope images (30X magnification) of spray-dried UFH (1A) and co spray-dried UFH with leucine (1%, w/w) (1B) at 0% RH. Images of spray-dried UFH (1A') and co spray-dried UFH with leucine (1%, w/w) (1B') and after 15 min exposure to 90% RH.

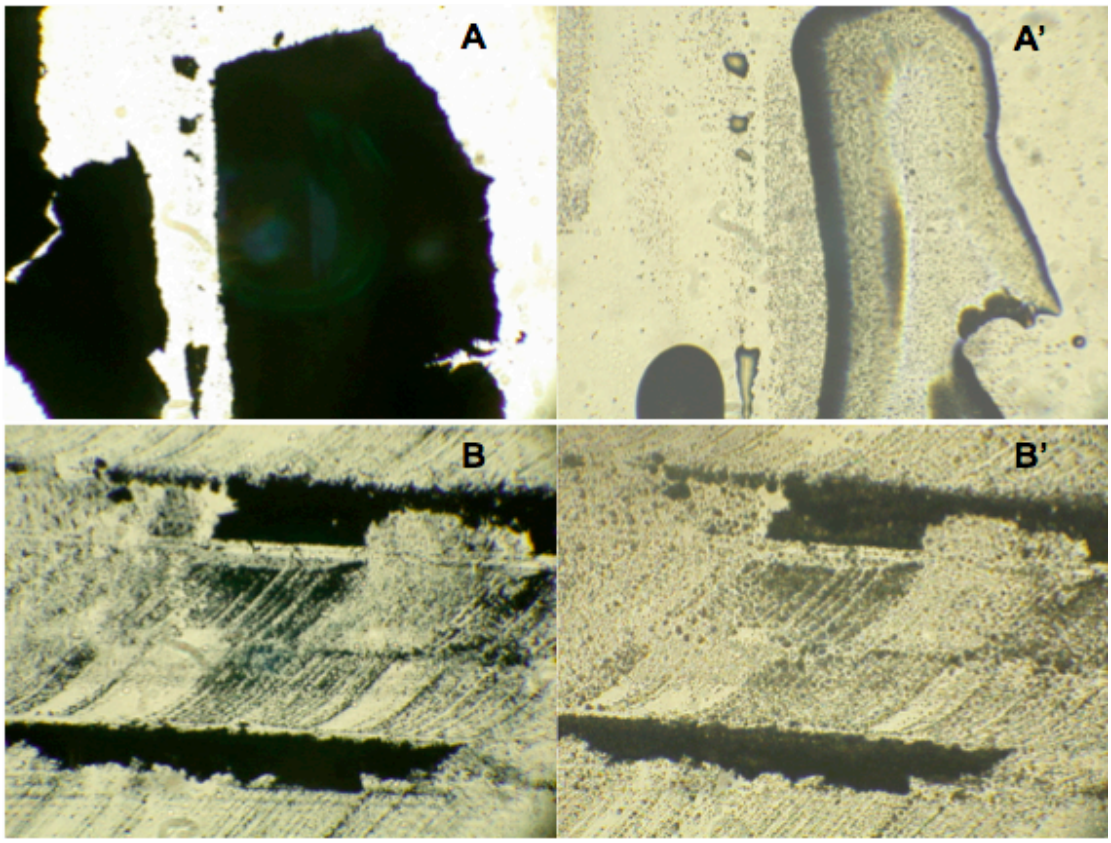

Figure 2. Scanning electron micrographs of engineered particles of budesonide produced by SAX using (A) ethanol, (B) acetone and (C) dichloromethane as the carrier solvent.

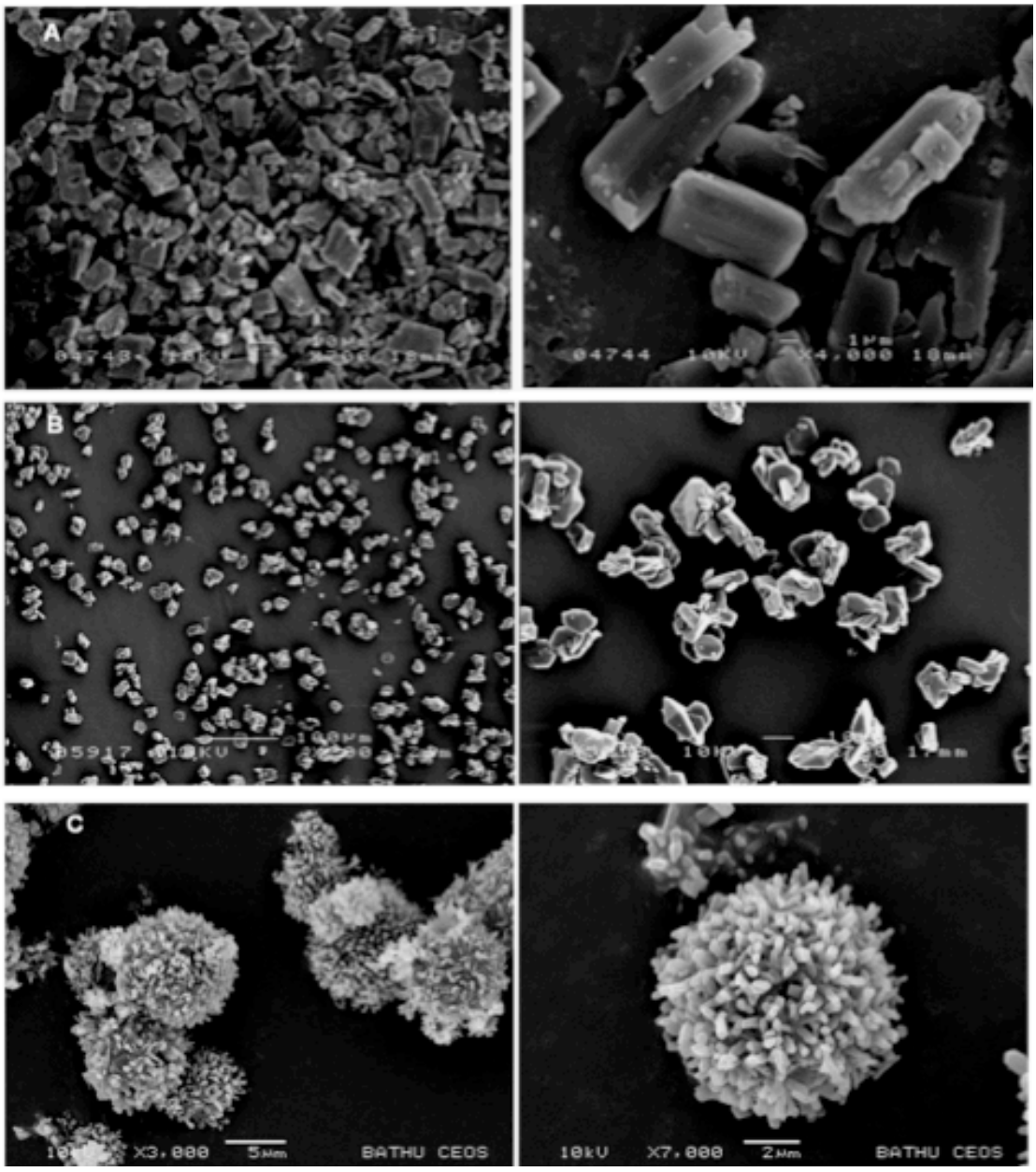

Figure 3. Scanning electron micrograph of a carrier based DPI formulation containing lactose monohydrate (SV003) and micronized budesonide.

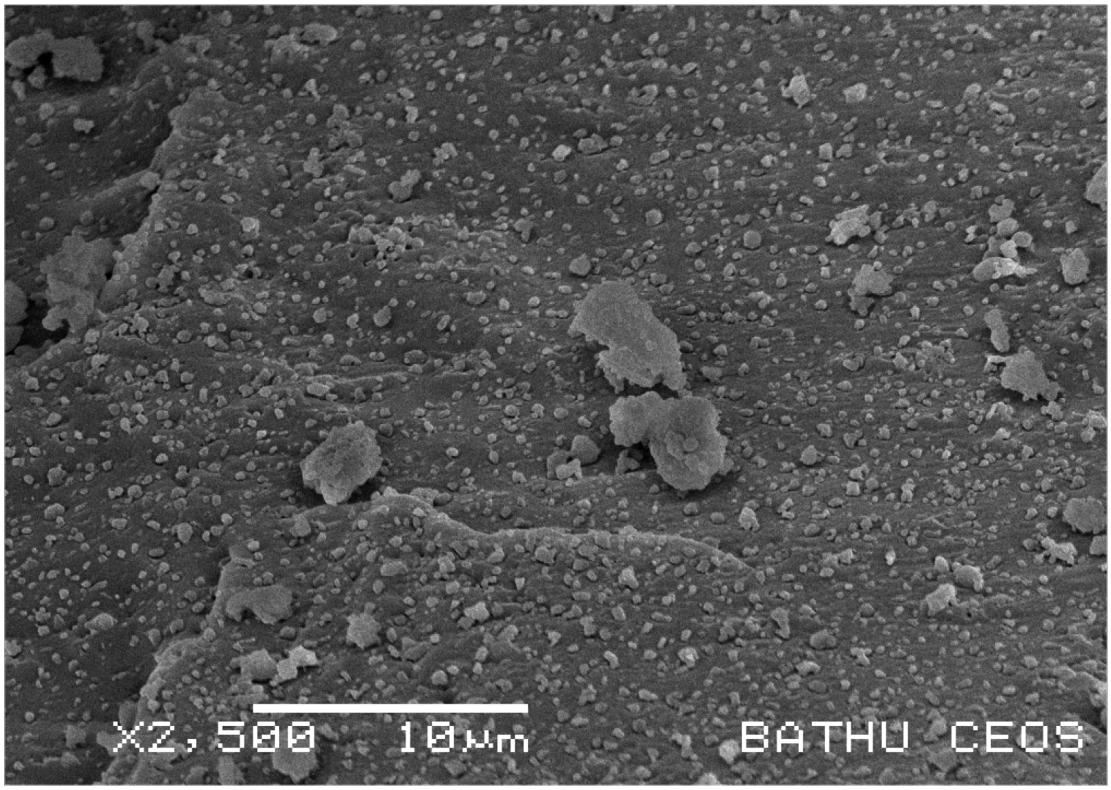

Figure 4. Colloid probe consisting of micronized salbutamol sulphate adhered to the apex of a V-shaped cantilever.

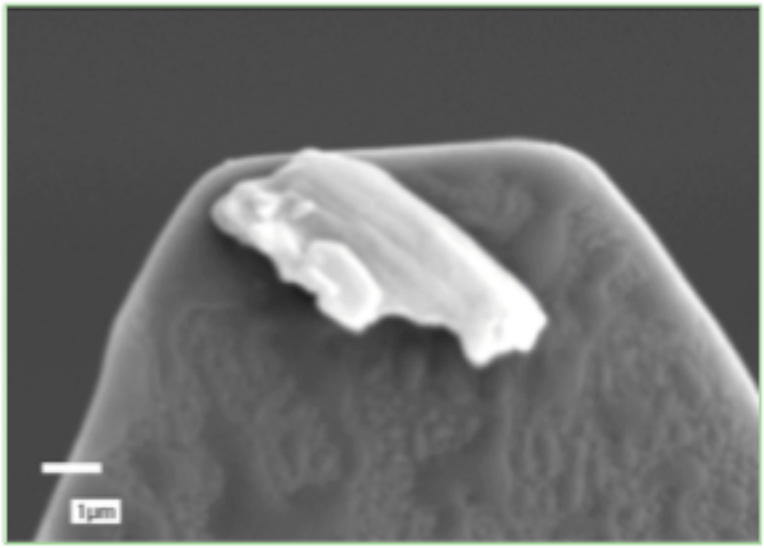

Figure 5. Representative force-volume images of ML001 (left) and SV003 (right). The area of each image is 20 μm x 20 μm and each pixel represents a force-distance measurements.

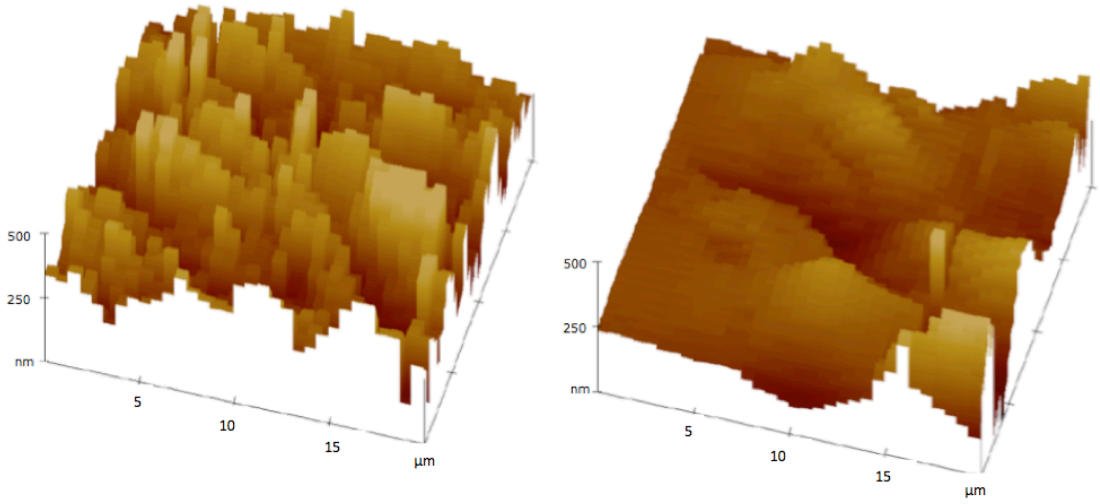

Figure 6. Topography (left) and Phase-image (right) of a particle of micronized salbutamol sulphate generated by TappingMode AFM.

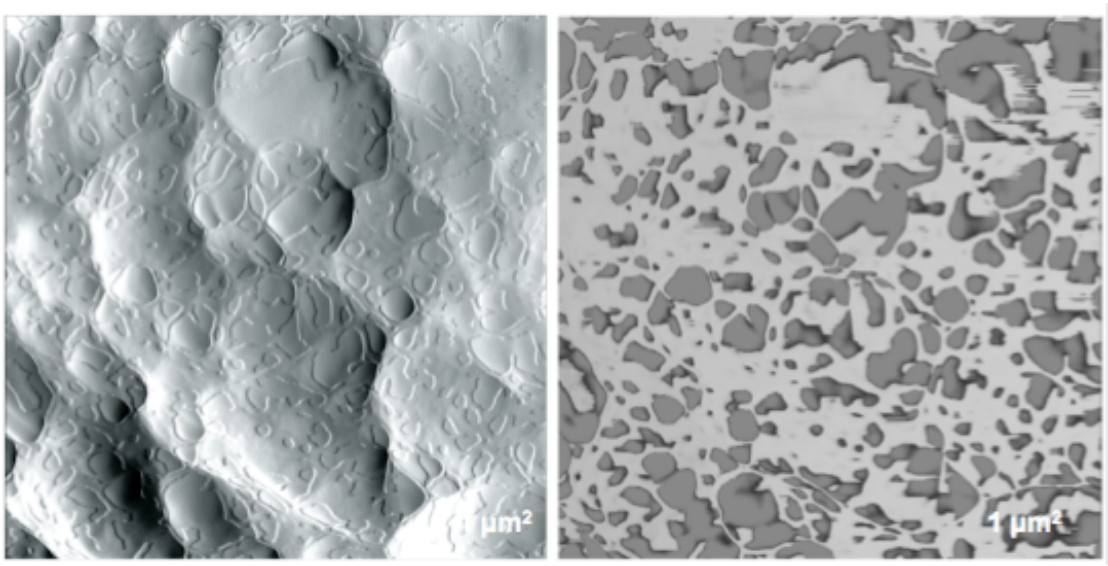

Figure 7. Surface of lactose particles of ML001 (milled lactose) using profilometry (A) by white light interferometry. (B) height image of the lactose particle.

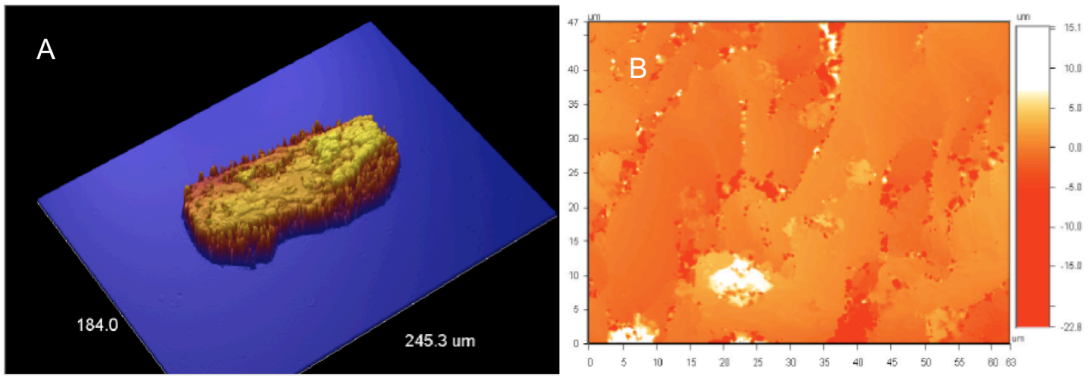

Figure 8. Bright-field reflectance (left) and Raman chemical image (right) of images of particles of fluticasone and lactose collected on stage 3 of the NGI following aerosolization of the Advair 500/50 DPI.